THE ASTROPHYSICAL JOURNAL, 439:279–287, 1995 January 20

EVIDENCE FOR CHEMICAL PROCESSING OF PRECOMETARY ICY GRAINS IN CIRCUMSTELLAR ENVIRONMENTS OF PRE–MAIN-SEQUENCE STARS

STEPHEN C. TEGLER,[1,2,3] DAVID A. WEINTRAUB,[2,3,4] TERRENCE W. RETTIG,[1,2,3]
YVONNE J. PENDLETON,[3,5] DOUGLAS C. B. WHITTET,[3,6] AND CRAIG A. KULESA[1,7]
Received 1994 May 19; accepted 1994 July 29

ABSTRACT

We report the detection of a broad absorption feature near 2166 cm^{-1} in the spectrum of the Taurus cloud source Elias 18. This pre–main-sequence source is the second in Taurus, the third in our survey, and the fifth known in the sky to show the broad 2166 cm^{-1} absorption feature. Of equal importance, this feature is not seen toward several other embedded sources in our survey, nor is it seen toward the source Elias 16, located behind the Taurus cloud. Laboratory experiments with interstellar ice analogs show that such a feature is associated with a complex C≡N containing compound [called X(C≡N)] that results from high-energy processing (ultraviolet irradiation or ion bombardment) of simple ice components into more complex, organic components. We find a nonlinear anticorrelation between the abundance of X(C≡N) and frozen CO in nonpolar lattices. We find no correlation between the abundance of X(C≡N) and frozen CO in polar lattices. Because the abundances of frozen CO and H_2O are strongly correlated with each other and with visual extinction toward sources embedded in and located behind the Taurus molecular cloud, these ice components usually are associated with intracloud material. Our results indicate that X(C≡N) molecules result from chemical processing of dust grains dominated by nonpolar icy mantles in the local environments of pre–main-sequence stars. Such processing of icy grains in the early solar system may be an important source of organic compounds observed in minor solar system bodies. The delivery of these organic compounds to the surface of the primitive Earth through comet impacts may have provided the raw materials for prebiotic chemistry.

Subject headings: circumstellar matter — dust, extinction — infrared: stars — ISM: individual (Taurus Dark Cloud) — ISM: molecules — stars: pre–main-sequence

1. INTRODUCTION

During the 20th century many exciting advances have taken place in planetary astronomy. Perhaps one of the most exciting advances was the discovery that meteorites, comets, and interplanetary dust particles are rich in large, complex carbon-bearing molecules. A carbon-bearing meteorite (carbonaceous chondrite) that fell near Murchison, Australia, in 1969 was observed to contain 74 different amino acids (Cronin, Pizzarello, & Cruickshank 1988), 19 of which occur biologically on Earth (Marcus & Olsen 1991). The *Giotto* and *Vega* spacecrafts to comet Halley discovered that the dust of comet Halley consisted of three components, one composed of only carbon, hydrogen, oxygen and nitrogen atoms (the so-called CHON grains), another composed of a magnesium-rich silicate without any significant organic material, and a third composed of a mixture of the first two components. The particle impact analyzer instruments PIA and PUMA aboard the *Giotto* and *Vega* spacecrafts discovered that the CHON grains accounted for 30% of the total dust mass analyzed (see reviews by Jessberger & Kissel 1991; McDonnell, Lamay, & Pankiewicz 1991). The presence of large organic molecules in minor solar system bodies has lead authors to speculate that the influx of such bodies on the surface of the primitive Earth may have played a key role in prebiotic chemistry and the origin of life (Chamberlin & Chamberlin 1908; Oro 1961; Delsemme 1984; Anders 1989; see review by Chyba & Sagan 1992).

The potential significance of large carbon-bearing molecules in minor solar system bodies emphasizes the importance of exploring their origins. Greenberg (1982) and Greenberg & Hage (1990) have proposed that cometary bodies in the early solar system formed by accretion of submicron-sized grains originating in the interstellar medium. These grains are thought to be coated with mantles containing organic molecules formed by the photolysis of ices. Extensive laboratory experiments have been carried out to simulate the production of large carbon-bearing molecules in interstellar and circumstellar environments (Moore et al. 1983; Lacy et al. 1984; Allamandola, Sandford, & Valero 1988; Tegler et al. 1993). In these experiments, precometary ice analogs were exposed to either ion bombardment or ultraviolet irradiation. The experimental results show that the ices undergo chemical changes as a result of this exposure. The ions and ultraviolet photons break molecular bonds and the resulting radicals combine to form more complex molecules. Moore et al. (1983) and Lacy et al. (1984) measured a broad absorption band at ~2166 cm^{-1} in the spectra of some ice mixtures after exposure to ion bombardment and ultraviolet irradiation, respectively. Lacy et al. found that the 2166 cm^{-1} absorption band is present only in ice mixtures containing carbon and nitrogen atoms, e.g., a CO and NH_3 ice mixture. Because a carbon atom triply bonded to a nitrogen atom has a stretching vibration that results in a

[1] Department of Physics and Astronomy, University of Notre Dame, Notre Dame, IN 46556.
[2] Visiting Astronomer, Infrared Telescope Facility, which is operated by the University of Hawaii under contract with the National Aeronautics and Space Administration.
[3] Visiting Astronomer, United Kingdom Infrared Telescope, which is operated by the Royal Observatory Edinburgh on behalf of the Science and Engineering Research Council.
[4] Department of Physics and Astronomy, Vanderbilt University, Nashville, TN 37235.
[5] NASA Ames Research Center, MS 245-6, Moffett Field, CA 94035.
[6] Department of Physics, Rensselaer Polytechnic Institute, Troy, NY 12180.
[7] Present address: Steward Observatory, University of Arizona, Tucson, AZ 85721.

2166 cm^{-1} absorption band, Lacy et al. concluded that the measured absorption band is due to an unidentified molecule containing a —C≡N or C≡N— group (i.e., a nitrile or isonitrile group) that they designated the X(C≡N) molecule.

The significance of C≡N bearing material in prebiotic chemistry can be appreciated from laboratory experiments of Matthews (1992). Matthews proposes that HCN polymers, whose infrared laboratory spectra show absorption signatures associated with both the C≡N overtone and fundamental stretch, form easily on solar system bodies. Matthews has suggested that the young Earth may have been covered with HCN polymers as a result of either cometary bombardment or terrestrial synthesis and that these polymers played a prominent role in the formation of proteinaceous structures and life. Widespread detection of C≡N bearing material in solar system bodies as well as in the circumstellar environments of pre–main-sequence stars may require researchers to further examine Matthew's controversial chemical recipe for prebiotic chemistry.

The literature contains several reports of solid C≡N detections in solar system objects. However, more recent and higher precision observations are calling some of these detections into question. In particular, near-infrared spectra of comets Panther (1981 II) and Bowell (1982 II) (Jewitt et al. 1982), the Uranian rings (Soifer et al. 1981), the dark hemisphere of the satellite Iapetus (Bell, Cruickshank, & Gaffey 1985), and the outer belt asteroids 773 Irmintraud, 368 Haidea, and 1172 Aneas (Bell et al. 1988; Cruickshank et al. 1991) all show an absorption band near 4545 cm^{-1}. Cruickshank et al. (1991) combine their near-infrared spectra of asteroids with the above near-infrared spectra and find a good comparison between the astronomical spectra and laboratory spectra of organic residues. These authors suggest that the identity of the 4545 cm^{-1} band is most likely the C≡N stretch first overtone. However, Luu, Jewett, & Cloutis (1994) find no trace of absorption near 4545 cm^{-1} in spectra of some of the same asteroids reported in Cruikshank et al. Davies, Sykes, & Cruikshank (1993) find an organic feature in the near-infrared spectrum of the asteroid 5145 Pholus. The feature appears narrower than the absorption feature attributed to X(C≡N) in the spectra of comets Panther & Bowell (Jewitt et al.). Presumably the surfaces of some minor solar system bodies may be partially covered with large organic molecules containing nitrile or isonitrile groups.

Very little work has been carried out to determine whether or not large organic molecules similar to those observed on the surfaces of minor solar system bodies also reside in the mantles of icy grains located in dense molecular clouds. Ten years ago Lacy et al. (1984) first identified a broad absorption band near 2166 cm^{-1}, the C≡N stretch fundamental, in the spectra of two embedded protostars, W33A and NGC 7583 IRS 9. Recently, our group has detected the C≡N band near 2166 cm^{-1} in spectra of the FU Orionis star L1551 IRS 5 (Tegler et al. 1993) and the T Tauri star RNO 91 (Weintraub et al. 1994). The mantles of icy grains located along lines of sight to these pre–main-sequence stars contain C≡N bearing molecules.

In this paper, we report on the initial results of our 2200–2100 cm^{-1} spectroscopic survey of pre–main-sequence stars. Our observations show that X(C≡N) molecules reside in the mantles of icy grains toward two pre–main-sequence stars embedded in the Taurus dense cloud, Elias 18 and L1551 IRS 5. The detection of X(C≡N) toward L1551 IRS 5 is a confirmation of our previous work (Tegler et al. 1993). Our observations do not show evidence for X(C≡N) molecules located along lines of sight toward other pre–main-sequence stars embedded in Taurus and other dense clouds. We also present observations of Elias 16, a field star located behind the Taurus cloud (Elias 1978a). This star does not show any evidence of absorption by X(C≡N) molecules located in intracloud material. The results presented here allow us to address two questions of importance to organic chemistry in the early solar system. First, are X(C≡N) molecules associated with volatile or more refractory ice-coated grains? Second, are X(C≡N) molecules located in intramolecular cloud material or circumstellar shells and disks around pre–main-sequence stars?

2. OBSERVATIONS

Our observations were obtained with the Cooled Grating Spectrometer 4 (CGS4) (Ramsay et al. 1993) and the United Kingdom Infrared Telescope (UKIRT) on Mauna Kea, Hawaii, during 1993 November and December. The CGS4 detector was a 58 × 62 InSb array. Observations were obtained with a 15″ east-west chop and a 3″ slit width. Chopping and nodding was carried out along the slit. The spectrometer was used in first order with a 150 line mm^{-1} grating, providing a resolving power of $\lambda/\Delta\lambda$ of $\simeq$1600. The total useful frequency interval was 2194–2105 cm^{-1}. Frequency calibration was obtained with a Krypton lamp.

We also obtained spectroscopic observations with the Cryogenic Array Spectrometer (CGAS) (Tokunaga, Smith, & Irwin 1987) and the NASA Infrared Telescope Facility (IRTF) on Mauna Kea, Hawaii during 1991 October, 1992 April, and 1992 August. CGAS is a grating spectrometer with a linear array of 29 working InSb detectors. The observations were obtained with a 2.″7 circular aperture and a 20″ east-west chop. The spectrometer, used in first order with grating B for 2187–2145 cm^{-1} and 2157–2107 cm^{-1} spectra, provided a resolving power of $\lambda/\Delta\lambda$ of $\simeq$1300. Frequency calibration was obtained with a Krypton lamp.

CGS4 and CGAS spectra were bias, and sky-subtracted. The spectrum of each target object was divided by the spectrum of a nearby bright star. By restricting the airmass difference between an object and a bright star to less than 0.10, we insured that telluric absorption features were accurately removed. To achieve a relative flux calibration, the spectrum of each object was then multiplied by a blackbody function appropriate for the associated bright star. In the case of CGAS spectra, we connected the 2187–2145 cm^{-1} spectra with the 2157–2107 cm^{-1} spectra by matching the overlapping portions in the 2150 cm^{-1} region. A continuum was fit to each object spectrum. The continuum, a linear function, was determined from the average frequencies and fluxes of data points at the blue and red ends of a spectrum. Finally, an optical depth spectrum was determined for each object from

$$\frac{I}{I_0} = e^{-\tau}, \quad (1)$$

where I is the relative flux at a particular frequency, I_0 is the continuum flux at the same frequency, and τ is the optical depth at that frequency. A log of the observations is given in Table 1. Figures 1–7 show the optical depth spectra for the CGS4 and CGAS data. We discuss these spectra in detail in § 3.2.

3. INTERPRETATION

3.1. *Laboratory Ice Analogs*

In this section we describe the results of laboratory ice analog experiments. Because we find that laboratory spectra of

TABLE 1

PARAMETERS FOR OBSERVATIONS

Object	Frequency Interval (cm^{-1})	Integration Time Per Spectrum (s)	Number of Spectra	Bright Star	Spectra
Elias 18	2194–2105	18	4	BS 1412	CGS4
	2187–2145	23	2	BS 1412	CGAS
	2157–2107	23	3	BS 1412	CGAS
L1551 IRS 5...	2194–2105	18	2	BS 1412	CGS4
	2187–2145	32	4	BS 1412	CGAS
	2157–2107	32	4	BS 1412	CGAS
Elias 16	2194–2105	18	2	BS 1412	CGS4
HL Tau	2194–2105	18	1	BS 1412	CGS4
PV Cep	2187–2145	12	6	BS 7805	CGAS
	2157–2107	16	3	BS 8162	CGAS
Elias 1–12	2187–2145	12	6	BS 8228	CGAS
	2157–2107	12	6	BS 8228	CGAS
Z CMa.....	2187–2145	40	1	BS 2943	CGAS
	2157–2107	10	5	BS 2943	CGAS

solid $X(C{\equiv}N)$ and CO match our astronomical spectra best, our remarks are limited to solid $X(C{\equiv}N)$ and CO experiments.

3.1.1. CO

Laboratory experiments by Hagen, Allamandola, & Greenberg (1980) show that frozen CO has an absorption band near 2140 cm^{-1}. Extensive experiments by Sandford et al. (1988) show that the CO band center, width, and intensity are sensitive to the composition of the matrix material surrounding the CO molecules as well as the thermal and radiation history of the ice. In general, a narrowband (full width at half-maximum [FWHM] ~ 5 cm^{-1}) with center near 2140 cm^{-1} results from absorption by CO molecules surrounded by a matrix dominated by nonpolar molecules, such as CO or CO_2 molecules. A broadband (FWHM ~ 10 cm^{-1}) with center near 2135 cm^{-1} results from absorption by CO molecules surrounded by a polar matrix, such as H_2O molecules. A thorough study of the frozen CO band from theoretical, laboratory, and astronomical perspectives can be found in Sandford et al. (1988) and Tielens et al. (1991).

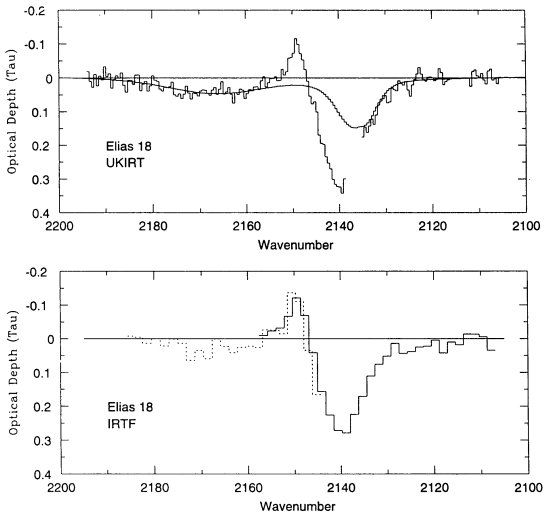

FIG. 1.—*Top panel:* UKIRT 2200–2100 cm^{-1} optical depth spectrum of Elias 18 (*solid line*). Laboratory ice analog spectrum (*dotted line*). *Bottom panel:* IRTF 2200 to 2100 cm^{-1} optical depth spectrum of Elias 18. The broad absorption band near 2166 cm^{-1} is attributed to solid $X(C{\equiv}N)$ molecules. The deep absorption band at 2140 cm^{-1} is associated with frozen CO molecules in nonpolar matrices. The absorption at 2135 cm^{-1} is due to frozen CO molecules in polar matrices. The emission feature at 2149 cm^{-1} is the Pfund-β hydrogen line and is probably photospheric in origin. The laboratory spectrum provides a good match to the $X(C{\equiv}N)$ band and the polar CO band. The lack of the 2140 cm^{-1} band in the laboratory spectrum is expected due to the polar nature of the matrix. Bad pixels are the cause of the gap in the UKIRT spectrum near 2137 cm^{-1}.

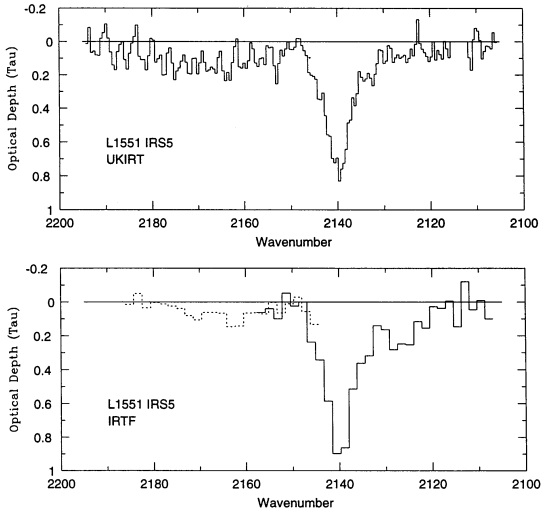

FIG. 2.—*Top panel:* UKIRT 2200–2100 cm^{-1} optical depth spectrum of L1551 IRS 5. *Bottom panel:* IRTF 2200–2100 cm^{-1} optical depth spectrum of L1551 IRS 5 (Reproduced from Tegler et al. 1993). The broad absorption band near 2166 cm^{-1} is attributed to solid $X(C{\equiv}N)$ molecules. The deep absorption band at 2140 cm^{-1} is associated with frozen CO molecules in nonpolar matrices. The absorption at 2135 cm^{-1} is due to frozen CO molecules in polar matrices.

3.1.2. $X(C{\equiv}N)$

Laboratory investigations of the chemical and thermal evolution of interstellar ice analogs are described in detail in Moore et al. (1983), Lacy et al. (1984), and Allamandola, Sandford, & Valero (1988). Here we briefly describe the laboratory experiment relevant to the comparison of laboratory and astronomical spectra in § 3.2. Tegler et al. (1993) present spectra of an interstellar ice analog (H_2O:CH_3OH:CO:NH_3 = 100:50:10:10) deposited at 10 K

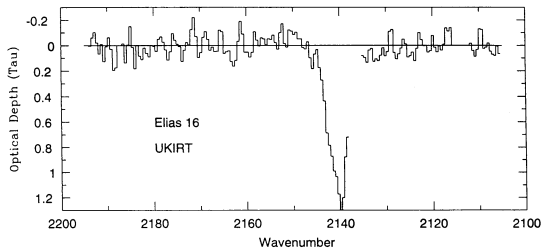

FIG. 3.—UKIRT 2200–2100 cm^{-1} optical depth spectrum of Elias 16. The deep absorption band at 2140 cm^{-1} is associated with frozen CO molecules in nonpolar matrices. A group of bad pixels obscure any measurements of the 2135 cm^{-1} band associated with frozen CO molecules in polar matrices.

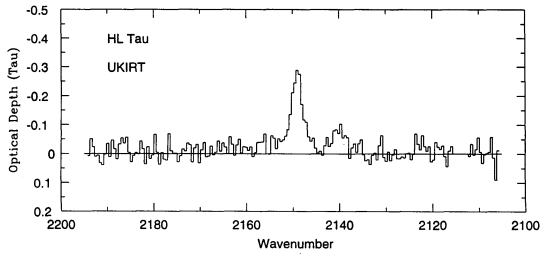

FIG. 4.—UKIRT 2200–2100 cm^{-1} optical depth spectrum of HL Tau. The emission feature at 2149 cm^{-1} is the Pfund-β hydrogen line and is probably photospheric in origin.

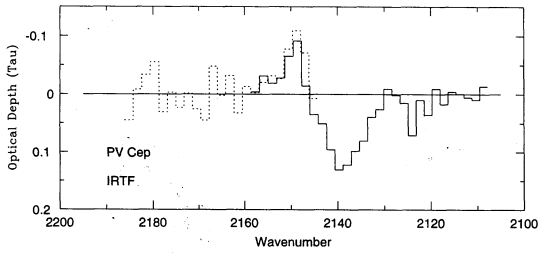

FIG. 5.—IRTF 2200–2100 cm^{-1} optical depth spectrum of PV Cep. The emission feature at 2149 cm^{-1} is the Pfund-β hydrogen line and is probably photospheric in origin. The deep absorption band at 2140 cm^{-1} is associated with frozen CO molecules in nonpolar matrices.

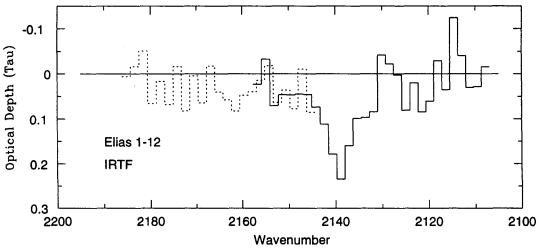

FIG. 6.—IRTF 2200–2100 cm^{-1} optical depth spectrum of Elias 1-12. The deep absorption band at 2140 cm^{-1} is associated with frozen CO molecules in nonpolar matrices. The absorption at 2135 cm^{-1} is due to frozen CO molecules in polar matrices.

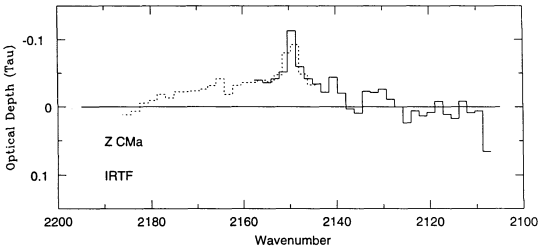

FIG. 7.—IRTF 2200–2100 cm^{-1} optical depth spectrum of Z CMa. The emission feature at 2149 cm^{-1} is the Pfund-β hydrogen line and is probably photospheric in origin.

with simultaneous photolysis for 15 hr. The spectra show that the $X(C\equiv N)$ band resulting from the photolysis has a central frequency that is temperature dependent. At 10 K the band peak is at 2168.4 cm^{-1} and steadily shifts to 2166.3 cm^{-1} at 100 K. At 150 K the band peak is at 2162.2 cm^{-1} when the ice has converted to cubic H_2O ice. Finally, after the H_2O ice sublimes, the $X(C\equiv N)$ band peak is at 2164.0 cm^{-1} in the refractory residue. In the discussion to follow we refer to the $X(C\equiv N)$ band center as near 2166 cm^{-1}. This is an approximate assignment as the exact assignment depends on the identity of the molecule and the temperature of the matrix.

3.2. *Comparison of Laboratory and Astronomical Spectra*

3.2.1. *Elias 18*

Elias 18 (Allen 1972; Elias 1978a) is the illuminating star of the reflection nebula IC 2087 in the Taurus dark cloud complex. It is a very red ($A_V = 17$, Elias 1978a; perhaps as low as $A_V = 12$, Whittet et al. 1988), low-luminosity (far-infrared luminosity of 0.86 $L_\odot$; Heyer, Snell, & Goldsmith 1987) object with no optical counterpart and no known spectral type; however, it does appear on the red print of the Palomar Sky Survey (Allen & Penston 1975). Thus, it appears to be a young stellar object in transition from embedded young stellar object stage to becoming a revealed T Tauri. The outflow associated with Elias 18 (Heyer et al.) is dominated by redshifted gas and is fairly old (1.9×10^5 yr) and weak ($L_{mech} = 8 \times 10^{-4}\ L_\odot$). Both the outflow age and energy are consistent with the idea that this source is in a transition stage.

Previous infrared spectroscopic observations show evidence for frozen H_2O and CO along the line of sight to Elias 18. Whittet et al. (1988) present spectra of Elias 18 that show strong absorption ($\tau = 0.80$) at 3275 cm^{-1} by frozen H_2O molecules. Sato et al. (1990) measure $\tau = 0.88$ for the same H_2O band. Whittet et al. (1985, 1989) present infrared spectra of Elias 18 that show absorption ($\tau = 0.35$) at 2140 cm^{-1} by frozen CO. With the benefit of 20/20 hindsight, we can see that the spectrum of Elias 18 in Whittet et al. (1985) shows a hint of the $X(C\equiv N)$ band near 2166 cm^{-1}. A spectrum of Elias 18 by Tielens et al. (1991) shows absorption due to frozen CO at 2139 cm^{-1} ($\tau = 0.39$) and 2136 cm^{-1} ($\tau = 0.15$). This spectrum does not cover the $X(C\equiv N)$ frequency interval.

We present in Figure 1 UKIRT and IRTF spectra of Elias 18 over the 2200–2100 cm^{-1} interval. Our UKIRT spectrum of Elias (solid line) reveals a broad (FWHM = 20 cm^{-1}) absorption band with maximum absorption ($\tau = 0.05$) near 2166 cm^{-1}, an emission feature with peak at 2149 cm^{-1}, and a narrow (FWHM = 10 cm^{-1}) absorption band with maximum absorption ($\tau = 0.34$) at 2140 cm^{-1}. The band at 2140 cm^{-1} appears somewhat asymmetric. Additional absorption ($\tau = 0.15$) appears to exist on the redward portion of the band (near 2135 cm^{-1}). Bad pixels are the cause of the gap in the spectrum near 2137 cm^{-1}.

The dotted line in Figure 1 is a spectrum of a laboratory ice analog deposited at 10 K and exposed to ultraviolet irradiation for 15 hr. The composition of the preirradiated ice was $H_2O:CH_3OH:CO:NH_3 = 100:50:10:10$, a composition chosen because its mid-infrared spectrum reproduces the main ice absorption features in the spectra of embedded objects such as W33A and NGC 7538 IRS 9. The CO and NH_3 concentrations are enhanced by a factor of 2–5 relative to the normal interstellar ice abundance to increase the $X(C\equiv N)$ yield and thereby facilitate its study. It is important to study the band

carrier in a realistic ice as matrix effects can produce significant spectral variations. A full description of the experimental procedure and equipment used to obtain this laboratory data can be found elsewhere (Allamandola et al. 1988). Two absorption bands are easily seen in the laboratory spectrum, $X(C\equiv N)$ near 2166 cm^{-1} and frozen CO in a polar matrix at 2135 cm^{-1}. Because CO molecules in the laboratory sample are in a polar matrix, absorption at 2140 cm^{-1} by CO molecules in a nonpolar matrix is not present. The laboratory spectrum is scaled so that the optical depth of the $X(C\equiv N)$ band center matches the optical depth of the band in the Elias 18 spectrum. From a comparison of the laboratory and Elias 18 spectra, we associate the 2166 cm^{-1} feature in the spectrum of Elias 18 with solid $X(C\equiv N)$; we associate the 2135 cm^{-1} feature with frozen CO in a polar matrix. The band at 2140 cm^{-1} in the spectrum of Elias 18 is consistent with frozen CO in a nonpolar matrix. Our observations of frozen CO are in excellent agreement with previous investigations of CO toward Elias 18. We associate the emission feature at 2149 cm^{-1} with the Pfund-β hydrogen line. We assume this line has a stellar origin. A comparison of the UKIRT and IRTF spectra in Figure 1 shows very good agreement. The constancy of the relatively weak $X(C\equiv N)$ band between two independent data sets taken with two different telescopes and spectrometers verifies the presence of the $X(C\equiv N)$ band.

3.2.2. *L1551 IRS 5*

IRS 5, which is the driving source for the extremely well separated, prototypical bipolar outflow in the dark cloud L1551, shows a K2 III or later spectral type (Carr, Harvey, & Lester 1987; Stocke et al. 1988), emits a modest bolometric luminosity of $\sim 40\ L_\odot$ (Stocke et al.), likely has a mass of less than $\sim 2.5\ M_\odot$ (Strom et al. 1985), and is shrouded by ≥ 19 mag of optical extinction (Snell et al. 1985; Cohen 1975; Davidson & Jaffe 1984) along our line of sight. The outflow lobes are well collimated from within 0".5 out to $\geq 10'$ (≥ 0.5 pc at a distance of 160 pc) from the central source (e.g., Bieging & Cohen 1985). These results suggest that L1551 IRS 5 is more evolved than typical protostars and is surrounded by a thick circumstellar disk, viewed nearly edge-on to the plane of the sky (Stocke et al. 1988). In fact, Mundt et al. (1985), Carr et al. (1987), and Stocke et al. (1988) have shown that L1551 IRS 5 is probably an FU Orionis star. Keene & Masson (1990) have found that L1551 IRS 5 has a larger than 2000 AU radius envelope surrounding a compact core. They suggest the core, which has a radius of 45 ± 20 AU and a column density of ~ 1000 g cm^{-2}, is the preplanetary disk inferred to exist around this star.

Previous investigations show evidence for frozen H_2O and CO toward L1551 IRS 5. Sato et al. (1990) show an infrared spectrum with strong ($\tau = 2.1$) absorption at 3275 cm^{-1} that they identify with frozen H_2O along the line of sight to L1551 IRS 5. Tielens et al. (1991) observe absorption at 2140 cm^{-1} ($\tau = 0.80$) and 2136 cm^{-1} ($\tau = 0.16$) that they identify with CO in nonpolar and polar matrices, respectively, along the line of sight to L1551 IRS 5.

In Figure 2 we present our UKIRT and IRTF spectra of L1551 IRS 5. Our UKIRT spectrum contains a broad (FWHM = 20 cm^{-1}) absorption band with maximum absorption ($\tau = 0.16$) near 2166 cm^{-1}, the $X(C\equiv N)$ band. The spectrum also contains a narrower (FWHM = 10 cm^{-1}) absorption band with maximum ($\tau = 0.83$) at 2140 cm^{-1} that we attribute to frozen CO in a nonpolar matrix. The low-frequency feature ($\tau = 0.23$) seen at 2135 cm^{-1} is due to frozen CO in a polar matrix. As in the case of Elias 18, our observations of frozen CO toward L1551 IRS 5 are in excellent agreement with previous investigations of CO toward this source. Our UKIRT spectrum in Figure 2 is in good agreement with our IRTF spectrum. The constancy of the relatively weak $X(C\equiv N)$ band between two independent datasets verifies the presence of the $X(C\equiv N)$ band.

We note that the high-frequency pattern superposed on the UKIRT spectrum of L1551 IRS 5 is the result of incomplete removal of absorption by telluric CO. We conclude the pattern is of telluric origin from our division of a spectrum of BS 1412 (the comparison star for L1551 IRS 5) by another spectrum of BS 1412. This division results in the same high-frequency seen in the spectrum of L1551 IRS 5. The pattern correlates closely with gas phase CO lines. Since BS 1412 (A7 III, $T_e = 8190$ K) is too hot for gaseous CO to exist in its photosphere, we conclude the pattern is of telluric origin. The airmass difference between the two BS 1412 observations as well as the L1551 IRS 5 and BS 1412 observations are somewhat larger than the object and comparison star airmass differences in the rest of the survey.

3.2.3. *Elias 16*

Elias 16 (Elias 1978a) is a K1 III field star located behind the Taurus dark clouds and viewed through $20^m.6$ of visual extinction (Elias 1978a). With a value of A_v that is 7 mag greater than the next most heavily obscured background source cataloged by Elias, Elias 16 has become a well-studied source, appearing in most surveys that attempt to probe ice and other solid features in and through the Taurus clouds. The optical depths of both the solid CO band (Whittet et al. 1989; Tielens et al. 1991) and the solid H_2O band (Whittet et al. 1983) for Elias 16 are strongly correlated with A_v. Such observations of Elias 16 and other background stars led Whittet et al. (1983) to conclude that most of the ices seen toward most Taurus sources are interstellar (intracloud) rather than circumstellar in origin (Whittet et al. 1983, 1988, 1989). Whittet et al. (1988) and Smith, Sellgren, & Tokunaga (1989) measured frozen H_2O optical epths (at 3250 cm^{-1}) of 1.60 and 1.21, respectively. Whittet et al. (1989) and Tielens et al. (1991) find frozen CO optical depths at 2140 cm^{-1} of 0.96 and 1.00, respectively.

Our spectrum of Elias 16 (Fig. 3) shows no evidence for $X(C\equiv N)$ absorption near 2166 cm^{-1} ($\tau \leq 0.05$). We do see evidence for absorption by frozen CO in a nonpolar matrix at 2140 cm^{-1} ($\tau = 1.2$). Bad pixels in the vicinity of 2135 cm^{-1} prevent us from saying anything about the presence of absorption by CO in a polar matrix.

3.2.4. *HL Tauri*

HL Tauri is one of the most intensively studied T Tauri stars in the sky and is very close on the plane of the sky to another source in our survey, L1551 IRS 5. This star is one of the first for which evidence existed suggesting the presence of a circumstellar disk seen nearly edge-on. Cohen (1975) detected the presence of H_2O ice absorption; later, Rydgren, Strom, & Strom (1976) reported absorption at 10 μm due to silicates. From frozen H_2O and silicate detections and far infrared photometry, Cohen (1983) suggested that the visual extinction toward HL Tau results largely from an edge-on circumstellar disk. Beginning in 1984, evidence began to accumulate from infrared imaging (Grasdalen et al. 1984), infrared speckle interferometry (Beckwith et al. 1984, 1989), infrared polarimetric imaging (Weintraub et al. 1992), millimeter interferometry (Beckwith et al. 1986; Sargent & Beckwith 1987, 1991) and

millimeter continuum measurements (Weintraub, Sandell, & Duncan 1989, 1990; Beckwith et al. 1990) for the edge-on disk model. In addition, HL Tauri has an optical jet (Mundt, Ray, & Buhrke 1988) that is nearly orthogonal to the long axis of the imaged dust and gas structure; i.e., the circumstellar disk.

We present in Figure 4 our 2200–2100 cm^{-1} spectrum of HL Tau. We see no evidence for solid $X(C{\equiv}N)$ ($\tau \leq 0.02$) or frozen CO ($\tau \leq 0.02$) absorption. The Pfund-β hydrogen line is present at 2149 cm^{-1}.

3.2.5. *PV Cephei*

PV Cep is an irregularly variable star (Cohen et al. 1981) that apparently drives a bipolar outflow (Levreault 1984). This star, which lies at the head of the cometary nebula GM 29 has been classified variously as a very young T Tauri star, an FU Orionis star, and a Herbig Ae/Be star. Van Citters & Smith (1989) discovered a strong 3275 cm^{-1} frozen H_2O absorption band in the spectrum of PV Cep. Because of the large column density of cold, well-shielded H_2O ice that is required to produce this band, van Citters & Smith suggest that the frozen H_2O forms in the outer parts of a dense disk seen edge-on. The clear spatial separation of the bipolar lobes of the PV Cep outflow lend strong support to this argument, although the H_2O ice may also lie along the line of sight through dark cloud material in front of PV Cep. At submillimeter and millimeter wavelengths, PV Cep is a fairly bright, compact (<8″ FWHM) source (Sandell & Weintraub 1994). If the long wavelength thermal emission arises from a disk, the low visual extinction (3.5–5.0; van Citters & Smith) and the high extinction implied by the long wavelength measurements suggest that the disk must be viewed nearly edge-on but must be extremely thin or warped in order to provide a relatively clear line of sight to the star.

In Figure 5 we present our 2200–2100 cm^{-1} spectrum of PV Cep. We see no evidence of any ($C{\equiv}N$) absorption near 2166 cm^{-1} ($\tau \leq 0.04$). We do see evidence of absorption ($\tau = 0.13$) at 2140 cm^{-1} by frozen CO molecules in a nonpolar matrix. A hint of the 2135 cm^{-1} band appears to induce a slight asymmetry in the 2140 cm^{-1} band. Because the FWHM for CO in a nonpolar matrix is ≤ 5 cm^{-1}, a FWHM of 8.7 cm^{-1} for the 2140 cm^{-1} band in the spectrum of PV Cep also suggests the 2135 cm^{-1} band is present. Frozen CO molecules in nonpolar and probably polar matrices are present toward PV Cep.

3.2.6. *Elias 1-12*

Elias 1-12 is a very red ($J-K = 2.65$; $A_V = 10$) FU Orionis variable in the IC 5146 dark cloud (Elias 1978b) that drives a 0.6 $M_\odot$ bipolar outflow (Levreault 1984; Evans et al. 1994). Infrared spectra of Elias 1-12 reveal a deep, broad H_2O ice absorption feature at 3275 cm^{-1} ($\tau_{H_2O} = 0.66$; Sato et al. 1990) as well as evidence for absorption by H_2O vapor (Sato et al. 1992). The large *IRAS*, submillimeter and millimeter fluxes toward Elias 1-12 suggest that the star is surrounded by a significant amount of dust (Weintraub, Sandell, & Duncan 1991).

Our spectrum of Elias 1-12 (Fig. 6) shows no evidence for solid $X(C{\equiv}N)$ absorption ($\tau \leq 0.04$). However, we do see evidence for absorption by frozen CO in both nonpolar ($\tau = 0.023$) and polar ($\tau = 0.10$) matrices.

3.2.7. *Z Canis Majoris*

Z CMa is an extremely luminous pre–main-sequence object. Though originally classified by Herbig (1960) as a Herbig Ae/Be star, Hartmann et al. (1989) have argued in favor of classifying it as an FU Orionis star. According to Hartmann et al., the object we call Z CMa is best described as a luminous pre–main-sequence accretion disk rotating around an unseen, 1–3 $M_\odot$ central object. The high mass ratio of disk to star suggests the Z CMa could be a fairly young object ($< 10^4$ yr). A series of near-infrared speckle measurements (Haas et al. 1993; Koresko et al. 1991) have resolved Z CMa and revealed that this source is a binary with a separation of 0.″10 at P.A. 122° with component luminosities of 640 $L_\odot$ and 3000 $L_\odot$. Koresko et al. suggest that the binary is surrounded by an extended circumbinary disk and that each component may have its own circumstellar disk. Haas et al. limit the size of any extended halo to less than a few tenths of an arcsecond. Poetzel, Mundt, & Ray (1989) reported a bipolar outflow from Z CMa that is traced by an 0.″16 optical jet and at least 15 Herbig-Haro objects and extends ~300″ in both the red and blue outflow directions at P.A. 60°. Recently, Evans et al. (1994) mapped the molecular gas in this outflow and found 0.9 $M_\odot$, most of it in the red wing.

Our 2200–2100 cm^{-1} spectrum of Z CMa (Fig. 7) shows no evidence for solid $X(C{\equiv}N)$ absorption ($\tau \leq 0.01$) or frozen CO absorption ($\tau \leq 0.01$). An emission band at 2149 cm^{-1}, the Pfund-β hydrogen line, is clearly present. A broad emission feature appears to exist between 2180 and 2140 cm^{-1}. Further observations of Z CMa are necessary to confirm the presence of this feature.

4. COLUMN DENSITIES

We can calculate column densities of ice components along lines of sight to survey objects from our absorption band measurements. In particular, the column density of an absorbing species is given by

$$N_x = \frac{\Delta v_x \tau_x}{A_x}, \qquad (2)$$

where x represents a molecular band, Δv_x represents the FWHM of the band, τ_x represents the optical depth at band center, and A_x represents the band intensity. Values for A_x and Δv_x for frozen H_2O, $X(C{\equiv}N)$, and CO are taken from laboratory experiments (Table 2). The values for Δv_x are in agreement with our astronomical spectra. The optical depths at band centers are taken from our astronomical spectra. In Table 3 we summarize frozen CO, $X(C{\equiv}N)$, and H_2O optical depth measurements and 1 σ upper limits for our data. We choose 1 σ upper limits because the $X(C{\equiv}N)$ band is very broad. A string of data points near the centroid of the $X(C{\equiv}N)$ band with $\tau = 1$ σ should be observable in our spectra. We also present in Table 3 optical depth measurements for other pre–main-sequence stars that exhibit evidence for solid $X(C{\equiv}N)$ containing material. The objects in Table 3 are

TABLE 2

MOLECULAR BAND PARAMETERS

Molecule	Band Center (cm^{-1})	$\Delta v_{1/2}$ (cm^{-1})	Band Intensity (cm^{-1} molecule^{-1})
H_2O[a]	~3275	~335	2×10^{-16}
$X(C{\equiv}N)$[a]	~2166	~20	$2–4 \times 10^{-17}$
CO (nonpolar)[b]	~2140	~6	1×10^{-17}
CO (polar)[b]	~2135	~10	1.7×10^{-17}

[a] H_2O and $X(C{\equiv}N)$ values from d'Hendecourt & Allamandola 1986.
[b] CO values from Sandford et al. 1988.

TABLE 3

OPTICAL DEPTHS

Object	τ_{XCN}	$\tau_{CO,2140}$	$\tau_{CO,2135}$	τ_{H_2O}
W33A	1.30[a]	1.20[b]	0.43[b]	>5.40[c]
NGC 7538 IRS 9	0.20[a]	2.60[b]	0.43[b]	3.28[c]
RNO 91	0.19[d]	0.33[d]	...	1.29[d]
L1551 IRS 5	0.16[e]	0.83[e]	0.23[e]	2.10[f]
Elias 18	0.05[e]	0.34[e]	0.15[e]	0.88[f]
Elias 16	<0.05[e]	1.20[e]	0.18[b]	1.60[g]
PV Cep	<0.04[e]	0.13[e]	...	0.44[h]
Elias 1–12	<0.04[e]	0.23[e]	0.10[e]	0.66[f]
HL Tau	<0.02[e]	<0.02[e]	<0.02[e]	0.85[g]
Z CMa	<0.01[e]	<0.01[e]	<0.81[e]	...

[a] Lacy et al. 1984.
[b] Tielens et al. 1991.
[c] Willner et al. 1982.
[d] Weintraub et al. 1994.
[e] This work.
[f] Sato et al. 1990.
[g] Whittet & Duley 1991.
[h] Van Citters & Smith 1989.

arranged in order of decreasing $X(C\equiv N)$ optical depth. In Table 4 we calculate the column density associated with each entry in Table 3 using equation (2) and the appropriate entries from Tables 2 and 3.

5. DISCUSSION

Now that measurements or upper limits exist for $X(C\equiv N)$ column densities toward 10 pre–main-sequence stars, we can address questions of importance to organic chemistry in the early solar system. For example, are $X(C\equiv N)$ molecules associated with volatile or more refractory ice-coated grains? Are $X(C\equiv N)$ molecules associated with intramolecular cloud material or circumstellar shells and disks around pre–main-sequence stars?

Ice components detected toward a pre–main-sequence star may reside in a circumstellar environment, foreground intramolecular cloud material, or a combination of these two environments. By observing a strong correlation between the amount of frozen material and the number of grains (e.g., τ_{H_2O} vs. visual extinction) toward *field* stars located behind the Taurus dark cloud, Whittet et al. (1988, 1989) have shown that the intramolecular cloud material contains significant amounts of frozen H_2O and CO. From their observations of *embedded* sources in the Taurus cloud (e.g., Elias 1 and Elias 7) Whittet et al. suggest that ice absorption in the spectra of at least some embedded pre–main-sequence stars in Taurus arises primarily in foreground intracloud material and not in circumstellar matter. In the case of Elias 18, the abundances of frozen H_2O and CO per unit visual extinction appear to be lower than expected for foreground intracloud material, suggesting sublimation of both molecules in the circumstellar environment and nearby intracloud environment of the star. An alternative possibility is that the estimate of visual extinction toward Elias 18 is too high (Whittet et al. 1988, 1989), in which case the frozen CO and H_2O molecules may reside exclusively in foreground intracloud material. The latter explanation is supported by the profile shape of the ice feature in Elias 18, which is essentially identical to that of the field star Elias 16 and consistent with amorphous ice at 23 K (Smith et al. 1989). In contrast, HL Tau shows evidence for modification of ices in its circumstellar environment. The profile of the 3275 cm^{-1} feature in HL Tau indicates that the ices are at least partially annealed, consistent with location in a warm circumstellar disk. The absence of a solid CO feature toward HL Tau further supports this conclusion.

TABLE 4

COLUMN DENSITIES[a]

Object	N_{XCN} (cm^{-2})	$N_{CO,2140}$ (cm^{-2})	$N_{CO,2135}$ (cm^{-2})	N_{H_2O} (cm^{-2})
W33A	6.5–13	7.2	2.5	>90
NGC 7538 IRS 9	1.0–2.0	16	2.5	55
RNO 91	0.95–1.9	2.8[b]	...	22
L1551 IRS 5	0.80–1.60	5.0	1.40	35
Elias 18	0.25–0.50	2.0	0.88	15
Elias 16	<0.5	7.2	...	27
PV Cep	<0.4	0.78	...	7.4
Elias 1–12	<0.4	1.4	0.59	11
HL Tau	<0.2	<0.1	<0.1	14
Z CMa	<0.1	<0.06	<0.06	...

[a] Multiply entry by 10^{17}.
[b] Both polar and nonpolar components.

Our survey provides strong evidence that $X(C\equiv N)$ molecules are associated with the icy grain component of dense molecular clouds. The results in Table 3 show that the five sources with $X(C\equiv N)$ detections also have strong ($\tau > 0.8$) H_2O ice detections and moderate to strong ($0.3 < \tau < 2.6$) solid CO detections. Of previously studied sources, W33A and NGC7538 IRS 9 (Lacy et al. 1984) are unique only in that they have very large column densities of frozen material. These large column densities made it possible for the last generation of infrared spectrometers to detect weak bands such as $X(C\equiv N)$ only in the brightest sources. The current generation, i.e., CGS 4, allows us to detect $X(C\equiv N)$ molecules in a broader sample. The additional $X(C\equiv N)$ detections suggest that photolytic or ion bombardment processing of simple ices is likely a common phenomenon.

When we look in detail at the optical depths of the various features (Table 3), we see that detection of simple ices (H_2O and CO) appears to be a necessary but not a sufficient condition for the detection of $X(C\equiv N)$ molecules in our sample. We also note that, where detected, the $X(C\equiv N)$ feature does not correlate very strongly in optical depth with either H_2O or CO. This behavior is consistent with the hypothesis that $X(C\equiv N)$ molecules are produced by photolysis or ion bombardment of simple ices in dark clouds. The best example of a nondetection of $X(C\equiv N)$ molecules in a line of sight with a large column density of ice grains is that of the Taurus background star Elias 16. The background star Elias 16 and the embedded source Elias 18 lie relatively close to one another on the plane of the sky and are heavily obscured with visual extinctions of 20.6 and 17 mag, respectively. Furthermore, Elias 16 and Elias 18 are of similar apparent brightness at 4.6 μm, $M = 3.9$, and $M = 3.4$, respectively (Elias 1978a). The individual spectra of Elias 16 and Elias 18 that were combined to produce the optical depth spectra in Figures 1 and 3 were obtained during a continuous 4 hr interval of time under uniform conditions. Since we were able to see evidence of $X(C\equiv N)$ absorption in the individual spectra of Elias 18 ($\tau = 0.05$), but not in the individual spectra of Elias 16, we conclude the upper limit of $X(C\equiv N)$ absorption toward Elias 16 is probably as small as $\tau < 0.05$. This result indicates that the intracloud material is deficient of $X(C\equiv N)$ molecules. In such regions, no processing has occurred, whereas toward embedded stars, the ice mantles have been at least partially

processed to form $X(C{\equiv}N)$ molecules. The strength of the 2166 cm^{-1} feature relative to the other ice signature depends on the nature and extent of the processing in a given line of sight.

Keeping in mind that $X(C{\equiv}N)$ is a processed ice, we note again that this processing must occur in dark cloud environments where high-energy photon or particle fluxes are available, i.e., around pre–main-sequence objects. Thus, *these results support the hypothesis that* $X(C{\equiv}N)$ *molecules form on grain surfaces around pre–main-sequence objects rather than in ambient, dark cloud material.*

It is important to determine whether $X(C{\equiv}N)$ is formed primarily in the polar or nonpolar component of the ice mantles. To investigate this question, we plot in Figure 8 $\tau(XC{\equiv}N)/\tau(H_2O)$ versus $\tau(CO)/\tau(H_2O)$ for both narrow and broad components of the CO feature. By normalizing to the water-ice feature, we are effectively plotting the abundance of $X(C{\equiv}N)$ against that of CO in polar and nonpolar ices, independent of the column density of icy material in individual lines of sight. The plot for nonpolar ices (Fig. 8*a*) shows a significant nonlinear anticorrelation. In contrast, there is no correlation in the plot for polar ices (Fig. 8*b*). The normalized strength of the polar CO feature is almost constant and does not show a tendency to be higher in lines of sight where $X(C{\equiv}N)$ is weak or absent. These results suggest that *it is the nonpolar ices that are being processed when* $X(C{\equiv}N)$ *is formed.*

By combining our results with a calculation of chemical processes in molecular clouds we can suggest a source of nitrogen necessary for the production of $X(C{\equiv}N)$ molecules. D'Hendecourt, Allamandola, & Greenberg (1985) present a calculation of grain mantle composition in molecular clouds as a function of time. The calculation includes an ion-molecule gas phase chemistry scheme, chemical reactions on grain surfaces, and continuous interaction between surface and gas phase molecules. Their calculation shows that at early times atomic hydrogen is abundant and that the atomic hydrogen combines with oxygen and nitrogen atoms on the grain surfaces to produce polar molecules such as H_2O and NH_3 in the mantles. As time proceeds, atomic hydrogen is converted to molecular hydrogen in the gas phase slowing the production of H_2O and NH_3 in the mantles. At later times nonpolar molecules such as CO, CO_2, O_2, and N_2 become more prominent in the mantles. Since our results indicate that $X(C{\equiv}N)$ molecules likely result from processing of nitrogen and carbon containing molecules in nonpolar mantles, the nitrogen source for the $X(C{\equiv}N)$ molecules is likely nonpolar N_2 rather than polar NH_3.

The apparent absence of $X(C{\equiv}N)$ molecules along the line of sight to HL Tau is very interesting. It is generally accepted that the ice absorption in this line of sight occurs primarily in an edge-on disk where the ice is partially annealed (§ 3.2.4). The circumstellar environment of HL Tau should be ideal for the modification of simple ices into $X(C{\equiv}N)$ molecules. The lack of detectable $X(C{\equiv}N)$ absorption cannot be readily explained by warm temperatures in the circumstellar disk since laboratory experiments show that $X(C{\equiv}N)$ molecules sublimate at a temperature (200 K) above the sublimation temperature of frozen H_2O (150 K). We argue above that $X(C{\equiv}N)$ forms by processing of the CO-dominated nonpolar ices, and it is therefore significant that solid CO is also undetected in HL Tau. It may be the case that, for some reason, formation of the nonpolar component of the mantles was inhibited in the environment of HL Tau. Another possibility is that the nonpolar ices (which sublime at $T > 30$ K) were warmed and evaporated at an early epoch, before they could be processed by photolysis or ion bombardment.

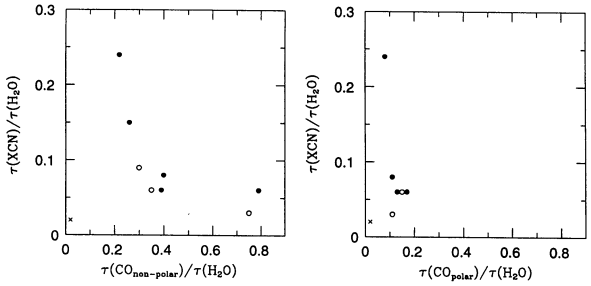

FIG. 8.—(*a*) Plot of $\tau(XC{\equiv}N)/\tau(H_2O)$ vs. $\tau(CO_{nonpolar})/\tau(H_2O)$ for sources in Table 3. Filled and open circles represent $X(C{\equiv}N)$ detections and upper limits, respectively. The cross represents HL Tau. (*b*) Plot of $\tau(XC{\equiv}N)/\tau(H_2O)$ vs. $\tau(CO_{polar})/\tau(H_2O)$ for sources in Table 3. The symbols are the same as in (*a*). The anticorrelation between $X(C{\equiv}N)$ and nonpolar CO (*a*) and the lack of any correlation between $X(C{\equiv}N)$ and polar CO (*b*) suggests nonpolar ices are being processed when $X(C{\equiv}N)$ is formed.

Our conclusions suggesting that (1) $X(C{\equiv}N)$ molecules are located in circumstellar environments around pre–main-sequence stars and (2) $X(C{\equiv}N)$ molecules result from chemical processing of nonpolar icy mantles are based on a limited amount of data. Additional observations of protostars, T Tauri stars, and background stars, in and behind Taurus, as well as additional laboratory experiments, are essential for determining the strength of our conclusions.

We thank Scott Sandford and Louis Allamandola for providing us with spectra of laboratory ice analogs. We also thank the staff astronomers and telescope operators at the United Kingdom Infrared Telescope and the NASA Infrared Telescope Facility for their advice and assistance in making the observations.

REFERENCES

Allamandola, L. J., Sandford, S. A., & Valero, G. J. 1988, Icarus, 76, 225
Allen, D. A. 1972, ApJ, 172, L55
Allen, D. A., & Penston, M. N. 1975, MNRAS, 172, 245
Anders, E. 1989, Nature, 342, 255
Beckwith, S. V. W., Sargent, A. I., Chini, R. S., & Güsten, R. 1990, AJ, 99, 924
Beckwith, S. V. W., Sargent, A. I., Koresko, C. D., & Weintraub, D. A. 1989, ApJ, 343, 393
Beckwith, S. V. W., Sargent, A. I., Scoville, N. Z., Masson, C. R., Zuckerman, B., & Phillips, T. G. 1986, ApJ, 309, 755
Beckwith, S. V. W., Zuckerman, B., Skrutskie, M. F., & Dyck, H. M. 1984, ApJ, 287, 793
Bell, J. F., Cruickshank, D. P., & Gaffey, M. J. 1985, Icarus, 61, 192
Bell, J. F., Owensby, P. D., Hawke, R. B., & Gaffey, M. J. 1988, in Lunar Planet. Sci. Conf., 19, 59
Bieging, J. H., & Cohen, M. 1985, ApJ, 289, L5
Carr, J. S., Harvey, P. M., & Lester, D. F. 1987, ApJ, 321, L71
Chamberlin, T. C., & Chamberlin, R. T. 1908, Science, 28, 897
Chyba, C., & Sagan, C. 1992, Nature, 355, 125
Cohen, M. 1975, MNRAS, 173, 229
———. 1983, ApJ, 270, L69
Cohen, M., Kuhi, L. V., Harlan, E. A., & Spinrad, H. 1981, ApJ, 245, 920
Cronin, J. R., Pizzarello, S., & Cruickshank, D. P. 1988, in Meteorites & the Early Solar Systems, ed. J. F. Kerridge & M. S. Matthews (Tucson: Univ. of Arizona Press), 819
Cruikshank, D. P., et al. 1991, Icarus, 94, 345
Davidson, J., & Jaffe, D. 1984, ApJ, 277, L13
Davies, J. K., Sykes, M. V., & Cruickshank, D. P. 1993, Icarus, 102, 166
Delsemme, A. H. 1984, Origins of Life, 14, 51

d'Hendecourt, L. B., & Allamandola, L. J. 1986, A&AS, 64, 453
d'Hendecourt, L. B., Allamandola, L. J., & Greenberg, J. M. 1985, A&A, 152, 130
Elias, J. H. 1978a, ApJ, 224, 857
———. 1978b, ApJ, 223, 859
Evans, N. J., III, Balkum, S., Levreault, R. M., Hartmann, L., & Kenyon, S. 1994, ApJ, 424, 793
Grasdalen, G. L., Strom, S. E., Strom, K. M., Capps, R. W., Thompson, D., & Castelaz, M. 1984, ApJ, 283, L57
Greenberg, J. M. 1982, in Comets, ed. L. L. Wilkening (Tucson: Univ. of Arizona Press), 131
Greenberg, J. M., & Hage, J. I. 1990, ApJ, 361, 260
Haas, M., Christou, J. C., Zinnecker, H., Ridgway, S. T., & Leinert, Ch. 1993, A&A, 269, 282
Hagen, W., Allamandola, L. J., & Greenberg, J. M. 1980, A&A, 86, 1-2
Hartmann, L., Kenyon, S., Hewett, R., Edwards, S., Strom, K., Strom, S., & Stauffer, J. 1989, ApJ, 338, 1001
Herbig, G. 1960, ApJS, 4, 337
Heyer, M. H., Snell, R. L., & Goldsmith, P. F. 1987, ApJ, 321, 370
Jessberger, E. K., & Kissel, J. 1991, in Comets in the Post Halley Era, ed. R. Newburn, M. Neugebauer, & J. Rahe (Dordrecht: Kluwer), 1075
Jewitt, D. C., Soifer, B. T., Neugebauer, G., Matthews, K., & Danielson, G. E. 1982, AJ, 87, 1854
Keene, J., & Masson, C. R. 1990, ApJ, 355, 635
Koresko, C. D., Beckwith, S. V. W., Ghez, A., Matthews, K., & Neugebauer, G. 1991, AJ, 102, 2073
Lacy, J. H., Baas, F., Allamandola, L. J., Persson, S. E., McGregor, P. J., Lonsdale, C. J., Geballe, T. R., & Van de Bult, C. E. P. 1984, ApJ, 276, 533
Levreault, R. M. 1984, ApJ, 277, 634
Luu, J., Jewitt, D., & Cloutis, P. 1994, AJ, in press
Marcus, J. N., & Olsen, M. A. 1991, in Comets in the Post-Halley Era, ed. R. Newburn, M. Neugebauer, & J. Rahe (Dordrecht: Kluwer), 439
Matthews, C. N. 1992, in Environmental Evolution, ed. L. Margulis & L. Olendzenski (Cambridge: MIT Press), 29
McDonnell, J. A. M., Lamy, P. L., & Pankiewicz, G. S. 1991, in Comets in the Post-Halley Era, ed. R. Newburn, M. Neugebauer, & J. Rahe (Dordrecht: Kluwer), 1043
Moore, M. H., Bertram, D., Khanne, R., & A'Hearn, M. F. 1983, Icarus, 54, 388
Mundt, R., Ray, T. P., & Bührke, T. 1988, ApJ, 333, L69
Mundt, R., Stocke, J., Strom, S. E., Strom, K. M., & Anderson, E. R. 1985, ApJ, 297, L41
Oro, J. 1961, Nature, 190, 389
Poetzel, R., Mundt, R., & Ray, T. P. 1989, A&A, 224, L13
Ramsay, S., Mountain, M., & Geballe, T. 1993, in Near-IR Spectroscopy: Future Observational Directions, ed. Sun Kwok (San Francisco: PASP Conf. Ser.), 41, 339
Rydgren, A. E., Strom, S. E., & Strom, K. M. 1976, ApJS, 30, 307
Sandell, G. S., & Weintraub, D. A. 1994, A&A, submitted
Sandford, S. A., Allamandola, L. J., Tielens, A. G. G. M., & Valero, G. J. 1988, ApJ, 329, 498
Sargent, A. I., & Beckwith, S. V. W. 1987, ApJ, 323, 294
———. 1991, ApJ, 382, L31
Sato, S., Nagata, T., Tanaka, M., & Yamamoto, T. 1990, ApJ, 359, 192
Sato, S., Okita, K., Yamashita, T., Mizutani, K., Shiba, H., Kobayashi, Y., & Takami, H. 1992, ApJ, 398, 273
Smith, R. G., Sellgren, K., & Tokunaga, A. T. 1989, ApJ, 344, 413
Snell, R. L., Bally, J., Strom, S. E., & Strom, K. E. 1985, ApJ, 290, 587
Soifer, B. T., Neugebauer, G., & Matthews, K. 1981, Icarus, 45, 612
Stocke, J. T., Hartigan, P. M., Strom, S. E., Strom, K. M., Anderson, E. R., Hartmann, L. W., & Kenyon, S. J. 1988, ApJS, 68, 229
Strom, S. E., Strom, K. M., Grasdalen, G. L., Capps, R. W., & Thompson, D. 1985, AJ, 90, 2575
Tegler, S. C., Weintraub, D. A., Allamandola, L. J., Sandford, S. A., Rettig, T. W., & Campins, H. 1993, ApJ, 411, 260
Tielens, A. G. G. M., Tokunaga, A. T., Geballe, T. R., & Baas, F. 1991, ApJ, 381, 181
Tokunaga, A. T., Smith, R. G., & Irwin, E. 1987, in Infrared Astronomy with Arrays, ed. C. G. Wynn-Williams & E. E. Becklin (Honolulu: Univ. of Hawaii), 367
van Citters, G. W., Jr., & Smith, R. G. 1989, AJ, 98, 1382
Weintraub, D. A., Kastner, J. H., Zuckerman, B., & Gatley, I. 1992, ApJ, 391, 784
Weintraub, D. A., Sandell, G., & Duncan, W. D. 1989, ApJ, 340, L69
———. 1990, BAAS, 22, 1265
———. 1991, ApJ, 382, 270
Weintraub, D. A., Tegler, S. C., Kastner, J. H., & Rettig, T. W. 1994, ApJ, 423, 674
Whittet, D. C. B., Adamson, A. J., Duley, W. W., Geballe, T. R., & McFadzean, A. D. 1989, MNRAS, 241, 707
Whittet, D. C. B., Bode, M. F., Longmore, A. J., Adamson, A. J., McFadzean, A. D., Aitken, D. K., & Roche, P. F. 1988, MNRAS, 233, 321
Whittet, D. C. B., Bode, M. F., Longmore, A. J., Baines, D. W. T., & Evans, A. 1983, Nature, 303, 218
Whittet, D. C. B., & Duley, W. W. 1991, Astron. Astrophys. Rev., 2, 167
Whittet, D. C. B., Longmore, A. J., & McFadzean, A. D. 1985, MNRAS, 216, 45P
Willner, S. P., et al. 1982, ApJ, 253, 174